1.0

1.1

1.25 1.4 1.6

4.5
50

2.8 2.5
3.2
3.6
4.0

2.2
2.0
1.8

MICROCOPY RESOLUTION TEST CHART
NATIONAL BUREAU OF STANDARDS 1963 A

F. G.

(12)

A Simple Model of a LINUS Fusion System with a Thick, Compressible, Resistive Liner

A. E. ROBSON

Plasma Physics Division

April 1977

NAVAL RESEARCH LABORATORY
Washington, D.C.

REPORT DOCUMENTATION PAGE		READ INSTRUCTIONS BEFORE COMPLETING FORM
1. REPORT NUMBER NRL Memorandum Report 3472	2. GOVT ACCESSION NO.	3. RECIPIENT'S CATALOG NUMBER
4. TITLE (and Subtitle) A SIMPLE MODEL OF A LINUS FUSION SYSTEM WITH A THICK, COMPRESSIBLE, RESISTIVE LINER.		5. TYPE OF REPORT & PERIOD COVERED Interim report on a continuing NRL problem
		6. PERFORMING ORG. REPORT NUMBER
7. AUTHOR(s) A. E. Robson		8. CONTRACT OR GRANT NUMBER(s)
9. PERFORMING ORGANIZATION NAME AND ADDRESS Naval Research Laboratory Washington, D.C. 20375		10. PROGRAM ELEMENT, PROJECT, TASK AREA & WORK UNIT NUMBERS NRL Problem H02-28F
11. CONTROLLING OFFICE NAME AND ADDRESS Office of Naval Research Arlington, Virginia 22217		12. REPORT DATE April 1977
		13. NUMBER OF PAGES 30
14. MONITORING AGENCY NAME & ADDRESS(if different from Controlling Office)		15. SECURITY CLASS. (of this report) UNCLASSIFIED
		15a. DECLASSIFICATION/DOWNGRADING SCHEDULE

16. DISTRIBUTION STATEMENT (of this Report)

Approved for public release; distribution unlimited.

NRL-MR-3472

17. DISTRIBUTION STATEMENT (of the abstract entered in Block 20, if different from Report)

18. SUPPLEMENTARY NOTES

19. KEY WORDS (Continue on reverse side if necessary and identify by block number)

Thermonuclear fusion
Flux compression
Megagauss fields

20. ABSTRACT (Continue on reverse side if necessary and identify by block number)

A simple model is developed to describe the compression of a plasma to high density and fusion temperature by a thick, compressible imploding liner. In contrast to previous thin liner calculations, the dwell time around peak compression is now less than the transit time of a sound wave through the liner, and thus only the inner part of the liner contributes to the inertial confinement of the plasma. The model first derives the size of the active part of the liner, and goes on to determine the final conditions (pressure, radius, etc.,) achieved by the compressible liner in terms of the same

(Continues)

DD $_{1 \text{ JAN } 73}^{\text{FORM}}$ 1473   EDITION OF 1 NOV 65 IS OBSOLETE
S/N 0102-014-6601

i

20. Abstract (Continued)

quantities derived from the incompressible model used previously. The effect of resistive diffusion of magnetic field into the inside surface of the liner is treated as a perturbation. Finally, the results of the model are used to determine the working point of a LINUS reactor.

CONTENTS

iii
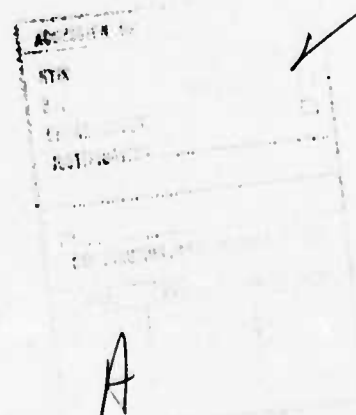
A SIMPLE MODEL OF A LINUS FUSION SYSTEM
WITH A THICK, COMPRESSIBLE, RESISTIVE LINER

I. Introduction

A simple model of the dynamic behavior of a cylindrical incompressible, perfectly-conducting liner imploding onto a $\beta = 1$ plasma was developed early in the LINUS program[1] in order to derive the basic scaling laws for power-producing systems. The principal relationship obtained was

$$Q = B_o r_o \rho^{\frac{1}{2}} P(b, T_o) \tag{1}$$

where Q = nuclear energy released in one cycle/plasma energy at peak compression;

$\quad$ B_o = buffer magnetic field between liner and plasma at peak compression (assumed of negligible extent);

$\quad$ r_o = minimum liner radius;

$\quad$ ρ = density of liner material;

$\quad$ T_o = plasma temperature at peak compression;

$\quad$ b = a dimensionless thickness parameter, defined by $A = \pi b^2 r_o^2$, where A is the cross-sectional area of the liner.

The function $P(b, T_o)$ was evaluated by integrating the thermonuclear reaction rate over a compression-expansion cycle (assumed symmetrical). It has a shallow maximum at $T_o = 20$ KeV, and varies with b as shown in Figure 1.

Note: Manuscript submitted March 24, 1977.

1

An important feature of the model was the description of the trajectory in time units of r_0/v_∞, where

$$v_\infty = \frac{B_0}{b} \left(\frac{3}{8\pi\rho}\right)^{\frac{1}{2}} \tag{2}$$

is the velocity of the liner if allowed to expand to infinity. The "dwell time" around peak compression during which reactions occur is then given by $\frac{r_0}{v_\infty} f(b)$.

In Reference 1, the effects of liner resistivity and compressibility were briefly considered. The effect of resistivity is to allow the buffer magnetic field to penetrate into the liner and thus some of the liner energy is dissipated that otherwise would go into plasma compression. Provided that the skin depth is small, the effect of resistivity may be treated as a perturbation, and the treatment of Reference 1 is still basically valid, although more detailed calculations in which the diffusion is incorporated self-consistently into the liner dynamics would lead to greater accuracy.

The effect of compressibility was also treated as a perturbation by assuming that all elements of the liner come to rest at peak compression and calculating the ratio E_c/E_0 of the energy stored in compression of liner material to the energy in the compressed plasma. A characteristic magnetic field B_1 was defined by $B_1^2 = 8\pi\rho c_s^2$, where c_s is the speed of sound in the liner material. Table 1 shows values of B_1 for some candidate liner materials. The fraction of energy in material compression was then given by

$$\frac{E_c}{E_0} = \frac{B_0^2}{B_1^2} g\ (b) \tag{3}$$

2

The function g is shown in Figure 2. For the thin liners (b ~ 3) that were being considered in the early stages of the LINUS program, the assumptions of the above treatment were justified provided $B_0 \leqslant B_1$.

The situation has changed drastically now that we are considering captive liquid liners which will be very thick (b ~ 30-40) at peak compression. Initial results from a one-dimensional fluid code[2] show that the inside surface comes to rest while the outside surface is still moving; the primary effect of compressibility is thus to modify the dynamics due to the finite speed of sound and to inhibit the transfer of energy from the outer regions of the liner to the inner regions on the time scale of the turnaround. The result is that the inside surface of the liner turns round at a larger radius and produces a lower peak plasma pressure than would have been anticipated by the incompressible model.

The purpose of this note is to describe a simple model which enables the actual turnaround radius r_* to be derived in terms of the turnaround radius r_0 anticipated by the incompressible model. The present model assumes that initially the liner motion can be predicted by the incompressible dynamics used previously, but that at some point in the compression cycle the liner can be divided into two regions, completely decoupled from each other. The outer region has no further effect on the inner region which executes a symmetrical compression-expansion trajectory, again determined by incompressible dynamics. The determination of the point of separation involves an adjustable parameter which may be used to fit the model to more exact numerical calculations. However, it will be shown that the results are relatively insensitive to this parameter, which leads us to believe that the model is

3

sufficiently accurate to be used in scaling studies and conceptual designs of LINUS systems.

II. The Model

The central feature of the model is the determination of the point of separation of the inner and outer regions of the liner. The liner position at the point of separation is shown in Figure 3. The radius of the inside surface is αr_*, the radius of the outside surface is r_2 and the radius of the surface of separation is $\tilde{r}$. The inner shell of the liner will eventually come to rest at radius r_*, which is of course greater than the radius r_0 at which the entire liner would have come to rest on the incompressible model.

Using the dimensionless thickness parameter b, defined in the Introduction, we have

$$r_2^2 = a^2 r_*^2 + b^2 r_0^2 \tag{4}$$

Similarly, we may define a thickness parameter b_* for the inner shell only

$$\tilde{r}^2 = a^2 r_*^2 + b_*^2 r_*^2 \tag{5}$$

The energy that will be delivered to the plasma when the inner shell comes to rest is

$$E_* = E_0 \left(\frac{r_0}{r_*}\right)^{2(\gamma-1)} \tag{6}$$

where E_0 is the total energy initially in the liner

$$E_0 = \tfrac{1}{2}\pi r_0^2 b^2 \rho v_\infty^2 \ . \tag{7}$$

4

Continuing the convention that starred quantities represent the values actually achieved by the compressible fluid we find

$$\frac{p_*}{p_0} = \left(\frac{r_0}{r_*}\right)^{2\gamma} \; ; \; \frac{B_*}{B_0} = \left(\frac{r_0}{r_*}\right)^{\gamma} \tag{8}$$

The energy that <u>has been delivered</u> to the plasma at the point of separation is

$$E_1 = E_0 \left(\frac{r_0}{ar_*}\right)^{2(\gamma-1)} \tag{9}$$

The energy <u>remaining to be delivered</u> is

$$E_2 = E_0 \left(\frac{r_0}{r_*}\right)^{2(\gamma-1)} \quad (1 - a^{-2(\gamma-1)}) \tag{10}$$

The energy <u>in the inner shell</u> of the liner is

$$E_3 = (E_0 - E_1) \, \ell n \, \frac{\tilde{r}}{ar_*} / \ell n \, \frac{r_2}{ar_*} \tag{11}$$

$$\simeq E_0 \left(1 - \left(\frac{r_0}{ar_*}\right)^{2(\gamma-1)}\right) \ell n \left(1 + \frac{b_*^2}{a^2}\right) / \ell n \left(1 + \frac{b^2 r_0^2}{a^2 r_*^2}\right)$$

Equating E_2 and E_3, and putting $S = \frac{r_*}{r_0}$, we obtain

$$(a^{2(\gamma-1)} - 1) \, \ell n \left(1 + \frac{b^2}{a^2 S^2}\right) = ((aS)^{2(\gamma-1)} - 1) \, \ell n \left(1 + \frac{b_*^2}{a^2}\right) \tag{12}$$

This equation may be used to obtain b_* as a function of S, with a and b as parameters.

We now define an <u>energy delivery time</u> as the time taken for the inner surface to go from ar_* to r_*

$$t_1 = \frac{r_*}{v_*} F(b_*, a, \gamma) \tag{13}$$

5

where F is obtained from the rather simple calculation of the incompressible trajectories described in Ref. (1). Since only the inner shell is involved, we have from (2)

$$v_*^2 = \frac{2p_*}{(\gamma-1)b_*^2 \rho} \tag{14}$$

We also define an <u>energy communication time</u>, as the time for a sound wave to travel from the outside to the inside of the inner shell:

$$t_2 = (\tilde{r} - ar_*)/c_s \approx r_* ((1 + b_*^2)^{\frac{1}{2}} - 1)/c_s \tag{15}$$

The assumption of incompressible motion of the inner shell is that $t_2 \leq t_1$. We now choose to <u>define</u> the point of separation by taking $t_2 = t_1$. Introducing a new parameter

$$\zeta = p_0/\rho c_s^2 = B_0^2/B_1^2 \tag{16}$$

which, as described in the Introduction, may be used as a measure of the degree to which compressibility must be considered, we obtain from equations (8) and (13) through (16)

$$(\gamma-1)b_*^2 \, S^{2\gamma}F^2(b_*, a, \gamma) = 2\zeta((1 + b_*^2)^{\frac{1}{2}} - 1)^2 \tag{17}$$

This equation may be used to obtain S as a function of b_*, with a and ζ as parameters. Given b, ζ and a, we may now use equations (12) and (17) to determine S and b_* by graphical methods. b and ζ characterize the <u>aimed-for</u> conditions in terms of the earlier incompressible model. S and b_* characterize the <u>achieved</u> conditions predicted by the current model, and all other relevant quantities may be derived from them.

6

III. Choice of α

The point of separation may be defined in terms of a fraction

$$f = \frac{\text{energy remaining to be delivered at point of separation}}{\text{total energy delivered at peak compression}}$$

which is related to the parameter α by

$$f = 1 - \alpha^{-2(\gamma-1)} \qquad (18)$$

As previously stated, α is an adjustable parameter which may be used to fit the results of the present model to the results of more exact hydrodynamic computations. A particular case for which computed results are available[2] is $b = 40$, $\zeta = 0.25$. We take these initial conditions and use the present model to derive S and b_* using four values of α, namely 1.18, 1.35, 1.68, and 2.28, which correspond to values of f of 0.20, 0.33, 0.50, and 0.67 respectively when γ is taken as 5/3. The results are shown in Table 2. Note that for $f < 0.5$, S varies by less than 1% from the value 1.32. b* increases steadily as f increases, as might be anticipated from simple physical considerations. The computed value of S is 1.57, which cannot be reconciled to our model simply by adjusting α. As will be shown in the next section, this discrepancy is resolved when the energy stored in compression of the liner material is taken into account.

It is difficult to estimate b* from the computed trajectory, since the latter is unsymmetrical with respect to the point of turnaround; however, $b* \sim 10$ provides a reasonably good fit. In all subsequent calculations, we shall therefore give α the value of 1.68, thus defining

the point of separation as the point where 50% of the final energy has been delivered to the plasma. Table 3 summarizes the results of 20 cases which cover the parameter range of practical interest and in addition to S and b_*, lists some other derived quantities.

IV. Correction for Material Compression

In the preceding discussion, the effect of compressibility was manifest only through the finite speed of sound which brought about the decoupling of the inner and outer shells of the liner. Since the inner shell is itself quite thick ($4 < b_* < 12$) it is necessary to take into account the energy stored in the compression of the liner material when calculating the motion of the inner shell. From equation (3) we find that the fraction of the inner shell energy stored in material compression when the shell comes to rest is

$$E_c/E_* = g(b_*)\zeta p_*/p_o \tag{19}$$

where g is the function shown in Fig. 2. E_c/E_* is tabulated on the bottom line of Table 3; it amounts to ~ 20-25% and thus represents a small but significant perturbation. Although, strictly speaking, the energy of compression should be incorporated self-consistently in the calculation of the motion, it is in keeping with the simple nature of our model to consider the effect only as a correction to the calculations already made. Subtracting the energy of compression from the energy of the plasma results in an increase in S by a factor $(1 - E_c/E_*)^{-0.75}$, with a corresponding effect on the derived quantities.

8

The corrected results are displayed in Table 4. Note that for our test case, $b = 40$, $\zeta = 0.25$, the model now predicts $S = 1.53$, compared to the computed value of 1.57. This remarkably good agreement, although probably fortuitous, gives one some confidence in the validity of the present model.

V. Thermonuclear Reactions

The thermonuclear yield is obtained by applying the analysis of Ref. 1 to a plasma compressed by the inner shell only. If Q is the ratio of the fusion energy yield to the energy E_o initially in the entire liner, and we neglect the energy in compression of liner material we have

$$Q = \frac{E'_*}{E_o} P(b_*, T_o) B'_* r'_* \rho^{\frac{1}{2}} = \left(\frac{E'_*}{E_o}\right)\left(\frac{B'_*}{B_o}\right) \zeta^{\frac{1}{2}} P(b_*, T_o) B_1 r'_* \rho^{\frac{1}{2}} \quad (20)$$

where P is the function shown in Fig. 1, B_1 is the characteristic field for the liner material given in Table 1, and the primes are used to indicate uncorrected values of the quantities.

The correction for material compression is made by taking the dwell time as unchanged, but multiplying the radius by $(1 - E_c/E'_*)^{-0.75}$ and the plasma density by $(1 - E_c/E'_*)^{1.5}$. Thus

$$Q = \left(\frac{E'_*}{E_o}\right) \left(\frac{B'_*}{B_o}\right) \zeta^{\frac{1}{2}} P(b_*, T_o)(1 - E_c/E'_*)^{2.25} B_1 r_* \rho^{\frac{1}{2}} \quad (21)$$

We now take $T_o = 20$ keV and construct a new function from equation 21,

$$P_*(\zeta, b) = Q/B_1 r_* \rho^{\frac{1}{2}} \quad (22)$$

P^* is also tabulated in Table 4. The units are the same as in Fig. 1.

9

Given ζ, b and the material constant $B_1\rho^{\frac{1}{2}}$ (Table 1), P_* enables the compressed plasma radius r_* to be determined for a given Q, and hence, through the other quantities listed in Table 4, the scale of the whole system.

An important quantity is the total (initial) liner energy per unit length E_o given by

$$E_o = \frac{3}{2} \cdot \frac{B_o^2}{8\pi} \cdot \pi r_o^2 = \frac{30}{16} \cdot \frac{\zeta Q^2}{\rho P_*^2 S^2} \ (MJ.m^{-1}) \tag{23}$$

For our present purpose it is convenient to express the energy in terms of a new quantity:

$$\hat{E}(\zeta,b) = E_o \rho / Q^2 \ (\rho \ \text{in gm.cm}^{-3}. \ E_o \ \text{in MJ.m}^{-1}) \tag{24}$$

values of which are included in Table 4.

As will be apparent in the next section, the time-scale for energy delivery t_1 is an important quantity, defined by equations (13) and (14). With $\alpha = 1.682$ and $\gamma = 5/3$ we have

$$t_1 = \frac{r'_*}{v_*} F(b_*) = \frac{r_*}{c_s} F(b_*) \left(\frac{b_* \ p_o}{\zeta \ p'_*} \right)^{\frac{1}{2}} \left(\frac{r'_*}{r_*} \right) \tag{25}$$

where, as previously, we assume that this time is not altered when material compression is taken into account. We may now construct a dimensionless time, as follows

$$\hat{t} \ (\zeta,b) = t_1 c_s / r_* \tag{26}$$

values of which are given in the last part of Table 4.

A number of interesting conclusions can be drawn from the results shown in Table 4. We note first that over the entire range of para-

10

meters studied (b = 10-50, ζ = 0.1-2.5), P_* varies by less than ±25%.
This means that, given the Q of the system and the liner material, the
compressed plasma radius r_* is almost independent of ζ and b. This is
in direct contrast to the prediction of the incompressible model,
namely that $r_o \propto B_o^{-1}$, which previously led us to believe that the
highest magnetic fields were desirable to reduce the radial dimension
of a LINUS fusion system. The incompressible model also predicted
that the energy per unit length $\hat{E}$ was independent of B_o, but the com-
pressible model indicates that $\hat{E}$ increases as ζ increases.

Clearly as ζ is reduced there must come a point $\zeta = \tilde{\zeta}(b)$ at which
the incompressible model becomes applicable; this point can be found
by putting S = 1, $b^* = b$ and $\zeta = \tilde{\zeta}$ in equation (17) and solving for $\tilde{\zeta}$.
Results are given in Table 5, which also lists P_* and $\hat{E}$ at $\zeta = \tilde{\zeta}$.
Although at this point sound transit effects are not important, material
compression must still be considered since although ζ is small, $b = b_*$
is large and $E_c/E_o \sim$ 10-15%. This correction has been applied in
calculating P_* and $\hat{E}$. The principal conclusion that can be drawn from
Table 5 is that in most cases of practical interest $\zeta > \tilde{\zeta}$ and so the
compressible model must always be used.

We conclude this section with a numerical example. Consider a
'breakeven' system (Q = 1) with a lead liner, and take ζ = 0.25, b = 40
as operating parameters. From Table 4, we find r_* = 3 cm and E_o =
23 MJ.m^{-1}. The peak magnetic field $B_* = 0.8$ MG. A system designed to
achieve fusion energy = plasma energy needs only Q = E_*/E_o = 0.57,
in which case r_* = 1.7 cm and E_o = 7.3 MJ.m^{-1}. These figures should
be compared with r_o = 1 cm and E_o = 14 MJ.m^{-1} derived in Ref. 1 for a

11

$Q = 1$ system with a thin copper liner at $B_o = 3$ MG.

VI. Effect of Finite Resistivity

The effect of compressibility is to reduce the efficiency of energy transfer from the liner to the plasma; the energy not delivered is stored in fluid motion and material compression and can, in principle, be recovered mechanically. On the other hand, the finite resistivity of the liner results in an irreversible loss of energy due to resistive dissipation of the flux-conserving current on the inside surface of the liner, and this energy appears as heat. As in Ref. 1, we shall treat this effect as a perturbation, that is, we shall assume $\delta/r_* \ll 1$, where δ is the skin depth. We assume that conditions at peak compression are not changed, and that the energy required to compensate for the dissipation is obtained by increasing the initial energy of the liner.

We are mainly interested in the total energy lost in a complete compression-expansion cycle, and so we assume that the inside surface of the liner is subjected to a magnetic pulse

$$B = B_* \sin (2\pi/T)t \tag{27}$$

and use the result of Knoepfel[3] that the energy skin depth at $t = T/2$ is given by

$$\delta = 1.27 \ (T/4\pi^2\sigma)^{\frac{1}{2}} \tag{28}$$

where σ is the electrical conductivity of the liner material (δ in cm, σ in e.m.u.).

The magnetic pulse at the liner surface is not in fact sinusoidal,

12

but the significant part of the pulse, which occurs between the point of separation and peak compression, can be approximated as a sine wave with fair accuracy, and this approximation is in keeping with the simple nature of our model.

At the point of separation

$$B = B_s = B'_* (1.682)^{-5/3} = 0.420 \, B_*(1 - f_c)^{-5/4} \qquad (29)$$

where $f_c = E_c/E'_*$. The matching to the sine wave is obtained by putting $t_1 = k_1 T/2\pi$, where t_1 is given by equation (25) and k_1 is given by

$$k_1 = \cos^{-1}(B_s/B_*) = \cos^{-1}(0.420 \, (1 - f_c)^{-5/4}) \qquad (30)$$

Thus

$$\delta = 1.27 \left(\frac{\hat{t} \, r_*}{2\pi k_1 \sigma c_s} \right)^{\frac{1}{2}} \qquad (31)$$

and substituting $r_* = Q/P_* B_* \rho^{\frac{1}{2}}$ and $B_1 = (8\pi\rho c_s^2)^{\frac{1}{2}} 10^{-6}$ (B_1 in MG) we obtain

$$\frac{\delta}{r_*} = \left(\frac{\rho 10^{-6}}{\sigma Q} \right)^{\frac{1}{2}} \cdot \left(\frac{1.29 P_* \hat{t}}{k_1} \right)^{\frac{1}{2}} = \left(\frac{\rho 10^{-6}}{\sigma Q} \right)^{\frac{1}{2}} \Delta(\zeta, b) \qquad (32)$$

The dimensionless quantity Δ is tabulated in Table 6. It varies by less than a factor of 2 over the range of parameters studied.

As an example, consider a system defined by $Q = 1$, $\zeta = 0.25$, $b = 40$ and take a lead liner ($\rho = 11.3$ gm.cm^{-3}) with a thin lithium layer ($\sigma = 2.10^{-5}$ e.m.u.) on the inside to carry the skin current.[4] Then $\delta/r_* = 0.2$, and so the effect of resistivity will be small, but significant. The energy lost is $E_*(2/3)(2\delta/r_*)$; the factor 2/3 arises because the lost energy is in magnetic field rather than plasma.

13

VII. LINUS Reactors

The principal purpose of the model developed here is to enable us to define and optimize the main physical parameters of a LINUS reactor system. Reduced to its essentials, a LINUS system consists of 1) an energy store (e.g., compressed gas), 2) the liner and 3) a magnetically confined plasma. A single cycle of the system proceeds as follows:

Compression

1. One unit of energy is taken from the store.

2. η_1 units are given to the liner as kinetic energy, $1 - \eta_1$ units are dissipated by fluid effects (e.g., viscosity).

3. $\eta_1(E_*/E_o)$ units are delivered to the plasma, $\eta_1 (1 - E_*/E_o)$ remain in the liner.

Reaction

4. $Q\eta_1$ units of fusion energy are produced, of which a fraction C is in α-particles that remain in the plasma and increase its energy to $\eta_1 (E_*/E_o + CQ)$ units.

Expansion

5. The plasma energy is given to the expanding liner, less $(\eta_1 E_*/E_o) \cdot (\frac{4}{3}\delta/r_*)$ units dissipated resistively.

6. The energy of the expanding liner, $\eta_1(1+CQ - \frac{E_*}{E_o} \cdot \frac{4}{3} \frac{\delta}{r_*})$ units, is returned to the store with efficiency η_2.

The mechanical cycle will be self-sustaining if the net energy taken from the store is zero, that is if

$$\eta_1\eta_2 \left(1 + CQ - \frac{E_*}{E_o} \cdot \frac{4}{3} \cdot \frac{\delta}{r_*}\right) - 1 = 0 \tag{33}$$

which may be written

14

$$CQ^{3/2} - (\frac{1}{\eta_1 \eta_2} - 1)Q^{\frac{1}{2}} - \frac{4}{3} (\frac{\rho 10^{-6}}{\sigma})^{\frac{1}{2}} \frac{E_*}{E_o} \cdot \Delta = 0 \qquad (34)$$

We make optimistic assumptions regarding the plasma, namely that it is $\beta = 1$, perfectly contained and that $C = 0.2$ (all α-particles trapped). We take a composite liner with the density of lead and the conductivity of lithium and, with $b = 40$, we solve equation (34) for Q as a function of ζ and the product $\eta_1 \eta_2$. The results are shown in Table 7. We see that for systems with very efficient fluid transfer ($\eta_1 \eta_1 \geq 0.9$), a self-sustaining reactor cycle is possible with $Q \leq 1$. We note also that Q decreases as ζ increases, but by less than a factor of 2 as ζ goes from 0.1 to 2.5. As an example, we choose $\zeta = 0.25$, $\eta_1 \eta_2 = 0.9$, giving $Q = 1.25$ and calculate the principal parameters of a LINUS reactor. The results are shown in Table 8. This choice of parameters conveniently leads to a liner thickness of ~ 100 cm at peak compression, which is a desirable thickness for neutron absorption and tritium breeding.

As we have seen throughout this report, the system parameters do not in general depend strongly on the choice of ζ. An exception is the energy per unit length E_o, and through this, the pressure required to drive the liner. Consider a captive liquid liner[2,4] driven by a constant external pressure p_{dr}. Since with this arrangement, the displacement of the liner equals its volume, we may equate the work done by p_{dr} to the liner energy E_o and obtain

$$b^2 p_{dr} = \zeta \left(\frac{B_1^2}{8\pi}\right) \frac{1}{\nu - 1} (1 + R) \qquad (35)$$

15

where R is the additional fraction of energy required for rotational stabilization.[2] Taking $R = 1$, $B_1 = 3.2$ MG (lead), $\gamma = 5/3$ we have

$$P_{dr} = 1.22\zeta/b^2 \text{ Mbars} \tag{36}$$

with $b = 40$ and $\zeta = 0.25$, equation (36) gives $p_{dr} = 190$ bars $= 2800$ psi, which is somewhat less than the steam pressures (~ 3500 psi) used in advanced thermal power plants.[5] Conversely, it might be argued that the engineering limit on driving pressure restricts the choice of ζ to ≤ 0.3.

Finally it should be said that the principal shortcoming of the model presented here is the assumption of a perfectly confined $\beta = 1$ plasma. To restrict end loss in a system of reasonable length it appears that a containment geometry with closed magnetic field lines will be necessary[2] and such systems generally have $\beta \leq 0.5$. A discussion of these systems is beyond the scope of this report but the effect on our results can at least be estimated.

The effect of $\beta < 1$ is to require that $P(b, T_o)$, equation (1) and Fig. 1, should be multiplied by a factor s, where $s \sim \beta^2 < 1$. Then from equations (20) to (22) we see that P_* must be multiplied by the same factor. Since P_* occurs again in equation (32), Δ must be multiplied by $s^{\frac{1}{2}}$, which in turn affects the value of Q derived from equation (34). If $\eta_1\eta_2 \approx 1$, $Q \propto \Delta^{2/3}$ and hence Q must be multiplied by $s^{1/3}$. Since $r_* \propto Q/P_*$, r_* must be multiplied by $s^{-2/3}$.

The principal consequence of $\beta < 1$ is therefore to increase the size of the system; some preliminary calculations by the author give $s \sim 0.25$ for a typical closed-field configuration. This would increase

16

r_* by 2.5 and the reactor outlined in Table 8 would become rather cumbersome. This study therefore indicates the need for plasma confinement with β as close as possible to unity.

VIII. References

1. A. E. Robson. Fundamental Requirements of a Fusion Feasibility Experiment Based on Flux Compression by a Collapsing Liner. NRL Memo Report 2616, July 1973.

2. D. L. Book, et al. Stabilized Imploding Liner Fusion Systems. 6th International Conference on Plasma Physics and Controlled Nuclear Fusion Research. Berchtesgaden FRG, 6-13 October 1976. Paper E-19-1.

3. H. Knoepfel. Pulsed High Magnetic Fields, North Holland-Elesevier, 1970, p. 77.

4. P. J. Turchi and A. E. Robson. Conceptual Design of Imploding Liner Fusion Reactors. Proc. 6th Symp. on Engineering Problems in Fusion Research, San Diego, Cal., Nov. 18-21, 1975, p. 983.

5. A Fusion Power Plant, R. G. Mills, ed., MATT-1050, Aug. 1974, p. 283.

TABLE 1

$$B_1 = (8\pi\rho c_s^2)^{\frac{1}{2}} \text{ and } B_1 \rho^{\frac{1}{2}}$$

Material	B_1 (MG)	$B_1 \rho^{\frac{1}{2}}$ (MG·gm$^{0.5}$·cm$^{-1.5}$)
Na	1.4	1.4
K	1.0	0.9
Li	1.8	1.3
Pb	3.2	10.8
Zn	4.0	10.7
Sn	3.7	10.0
Cu	5.6	16.7
Al	4.3	7.1
Hg	2.6	9.6

TABLE 2

α	1.182	1.355	1.682	2.280
f	0.20	0.33	0.50	0.67
S	1.32	1.33	1.31	1.24
b_*	3.0	4.8	7.8	13.0

TABLE 3: <u>Results uncorrected for material compression</u>

$\zeta =$	0.1	0.25	1.0	2.5
		$b = 10$		
S	1.03	1.12	1.31	1.47
b_*	8.4	5.8	3.5	2.6
P_*/P_o	0.91	0.69	0.41	0.28
E_c	0.19	0.22	0.26	0.29

$\zeta =$	0.1	0.25	1.0	2.5
		$b = 20$		
S	1.12	1.22	1.43	1.60
b_*	10.1	6.8	4.1	3.1
P_*/P_o	0.69	0.52	0.30	0.21
E_c	0.19	0.20	0.24	0.28

$\zeta =$	0.1	0.25	1.0	2.5
		$b = 30$		
S	1.17	1.28	1.49	1.68
b_*	10.7	7.4	4.4	3.3
P_*/P_o	0.59	0.44	0.26	0.18
E_c	0.17	0.19	0.23	0.26

$\zeta =$	0.1	0.25	1.0	2.5
		$b = 40$		
S	1.20	1.31	1.54	1.72
b_*	11.3	7.8	4.7	3.5
P_*/P_o	0.54	0.41	0.24	0.16
E_c	0.17	0.19	0.23	0.25

$\zeta =$	0.1	0.25	1.0	2.5
		$b = 50$		
S	1.23	1.34	1.57	1.76
b_*	11.7	8.1	4.8	3.6
P_*/P_o	0.50	0.38	0.22	0.15
E_c	0.16	0.17	0.22	0.25

TABLE 4: Results corrected for material compression

(a) Table of $S = r_*/r_o$

ζ \ b	10	20	30	40	50
0.1	1.21	1.31	1.35	1.38	1.40
0.25	1.35	1.44	1.50	1.53	1.54
1.0	1.64	1.76	1.81	1.87	1.89
2.5	1.90	2.05	2.11	2.13	2.18

(b) Table of b_*

ζ \ b	10	20	30	40	50
0.1	8.4	10.1	10.7	11.3	11.7
0.25	5.8	6.8	7.4	7.8	8.1
1.0	3.5	4.1	4.4	4.7	4.8
2.5	2.6	3.1	3.3	3.5	3.6

(c) Table of B_*/B_o

ζ \ b	10	20	30	40	50
0.1	0.73	0.64	0.61	0.58	0.57
0.25	0.61	0.54	0.51	0.49	0.49
1.0	0.44	0.39	0.37	0.35	0.35
2.5	0.34	0.30	0.29	0.28	0.27

TABLE 4   (Con't.)

(d)   Table of p_*/p_o

ζ \ b	10	20	30	40	50
0.1	0.53	0.41	0.37	0.34	0.33
0.25	0.37	0.30	0.26	0.24	0.24
1.0	0.19	0.15	0.14	0.12	0.12
2.5	0.12	0.09_1	0.08_3	0.08_0	0.07_4

(e)   Table of E_*/E_o

ζ \ b	10	20	30	40	50
0.1	0.78	0.70	0.67	0.65	0.64
0.25	0.67	0.61	0.58	0.57	0.56
1.0	0.52	0.47	0.45	0.43	0.43
2.5	0.42	0.38	0.37	0.36	0.35

(f)   Table of B_*/B_1

ζ \ b	10	20	30	40	50
0.1	0.23	0.20	0.19	0.18	0.18
0.25	0.30	0.27	0.25	0.25	0.24
1.0	0.44	0.39	0.37	0.35	0.35
2.5	0.54	0.48	0.46	0.45	0.43

TABLE 4   (Con't.)

(g) Table of P_*

ζ \ b	10	20	30	40	50
0.1	0.037	0.030	0.029	0.027	0.026
0.25	0.038	0.033	0.030	0.028	0.028
1.0	0.036	0.031	0.029	0.027	0.026
2.5	0.032	0.028	0.026	0.025	0.024

(h) Table of $\hat{E}$

ζ \ b	10	20	30	40	50
0.1	$9.1\ 10^1$	$1.2\ 10^2$	$1.2\ 10^2$	$1.3\ 10^2$	$1.4\ 10^2$
0.25	$1.8\ 10^2$	$2.1\ 10^2$	$2.3\ 10^2$	$2.5\ 10^2$	$2.5\ 10^2$
1.0	$5.4\ 10^2$	$6.3\ 10^2$	$6.8\ 10^2$	$7.4\ 10^2$	$7.8\ 10^2$
2.5	$1.3\ 10^3$	$1.4\ 10^3$	$1.6\ 10^3$	$1.6\ 10^3$	$1.7\ 10^3$

(i) Table of $\hat{t}$

ζ \ b	10	20	30	40	50
0.1	2.2	2.4	2.6	2.7	2.8
0.25	1.7	1.9	2.0	2.1	2.2
1.0	1.1	1.3	1.4	1.4	1.5
2.5	0.8_5	1.0	1.1	1.1	1.2

TABLE 5:   Limits of incompressible model

b	10	20	30	40	50
$\tilde{\zeta}$	0.066	0.020	0.010	0.006	0.004
P_*	0.036	0.025	0.020	0.017	0.014
$\hat{E}$	71	48	38	33	32

TABLE 6:   Table of $\Delta(\zeta, b)$

ζ \ b	10	20	30	40	50
0.1	0.32	0.31	0.31	0.30	0.30
0.25	0.29	0.29	0.28	0.27	0.28
1.0	0.24	0.24	0.23	0.23	0.23
2.5	0.20	0.20	0.21	0.20	0.20

TABLE 7:   Q for a mechanically self-sustaining reactor cycle

   $b = 40$, $C = 0.2$, lead liner

$\eta_1 \eta_2$ \ ζ	0.1	0.25	1.0	2.5
1.0	0.99	0.85	0.63	0.51
0.9	1.40	1.25	1.04	0.94
0.8	1.96	1.82	1.64	1.55
0.7	2.74	2.62	2.46	2.38

TABLE 8

Parameters of a LINUS reactor operating with a

self-sustained mechanical cycle

.

Dimensionless parameters: $\zeta = 0.25$

$b = 40$

$Q = 1.25$

$\eta_1 \eta_2 = 0.9$

Liner material: $B_1 = 3.2$ MG (lead)

$\rho = 11.3$ gm cm^{-3} (lead)

$\sigma = 2.10^{-5}$ e.m.u. (lithium)

Derived quantities: $r_* = 4.15$ cm (compressed plasma radius)

$r_2 = 108$cm (liner outer radius)

$B_* = 800$ kG (peak magnetic field)

$E_o = 36$ MJ.m^{-1} (liner energy, excluding rotation)

$E_f = 45$ MJ.m^{-1} (fusion energy)

$t_1 = 40$ μsec ($\sim \frac{1}{2}$ dwell time)

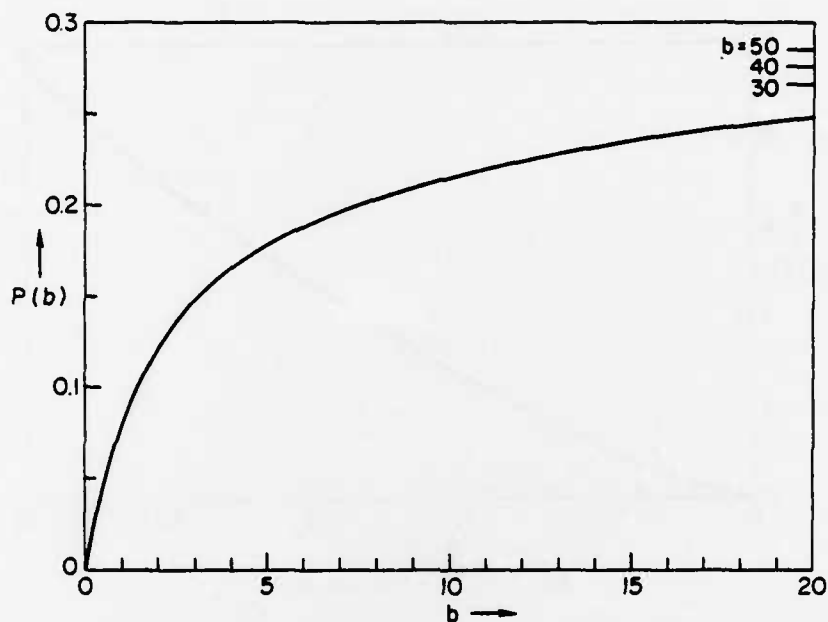$P_{dr} \approx 2800$ psi (driving pressure, including rotation)

Fig. 1 — $P(b) = Q/B_o r_o \rho^{1/2}$ as a function of b. $T_o = 20$ keV. B_o in MG, r_o in cm, ρ in gm.cm^{-3}. Each D-T reaction yields 17.6 MeV.
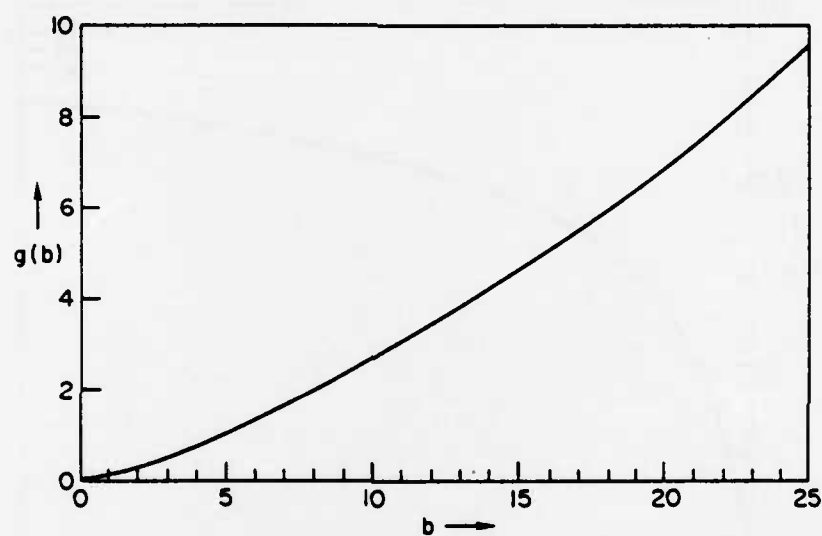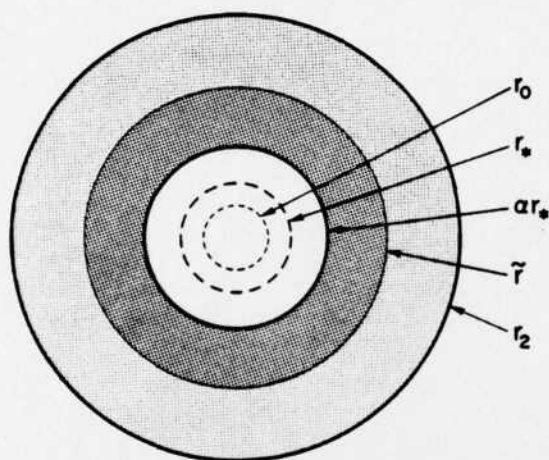
Fig. 2 — g as a function of b

26

Fig. 3 — Position of liner at point of separation